Synthetic Temperature Profile in the Gulf of Mexico:

Part I. Statistical Relationship Between Modal Amplitudes and Dynamic Height at Surface

D. S. Ko
Institute for Naval Oceanography
Stennis Space Center, MS 39529

May 1992

SYNTHETIC TEMPERATURE PROFILE IN THE GULF OF MEXICO:

PART I. STATISTICAL RELATIONSHIP BETWEEN MODAL AMPLITUDES AND DYNAMIC HEIGHT AT SURFACE

D. S. Ko

Institute for Naval Oceanography
Stennis Space Center, MS 39529

May 1992

TABLE OF CONTENTS

1. Introduction

The feasibility of estimating temperature profiles (synthetic temperature profiles) from Geodetic Earth Orbiting Satellite (GEOSAT) altimeter-derived sea-surface heights in the Gulf Stream region has been explored by Carnes et al (1990). The scheme was based on a statistical relationship between sea-surface heights (dynamic height at the surface relative to 1000 dbar) and subsurface temperature profiles derived by deWitt (1987). By analysis of the U.S. Navy's Master Oceanographic Observation Data Set (MOODS) hydrocast data in the Gulf Stream and Kuroshio regions, deWitt found that the first two empirical orthogonal functions (EOFs) of the temperature profiles represented more than 95 percent of the overall temperature variance. Furthermore, he found that there is a tight relationship between relative dynamic height and amplitude of the first two EOF modes. This relationship was used by Carnes et al to generate the synthetic temperature profiles from GEOSAT data. The synthetic temperature profiles compared well with the expendable bathythermograph (XBT) measurements.

In this study the temperature and salinity profiles in the Gulf of Mexico were collected and analyzed. Then the deWitt scheme was employed. The feasibility of using sea-surface heights to estimate temperature profiles (synthetic profiles) in the Gulf of Mexico was investigated.

2. Data

The data used in this study were obtained from 1) a quality-controlled version of the National Oceanographic Data Center (NODC) Oceanographic Station Data (SD) file (Levitus, 1982); 2) the U.S. Navy's MOODS; and 3) conductivity-temperature-depth (CTD) profiles from NODC which are not in the SD file or MOODS. The NODC SD file contained values of temperature, salinity, and dissolved oxygen at NODC standard depths. Temperature and salinity data were used as in the analysis.

The MOODS contains mostly XBT profiles which cannot be used due to 1) no salinity measurement and 2) no data deeper than 700 meters. Some CTD profiles were available in the MOODS and were used in the analysis. CTD data from MOODS were quality-controlled and re-sampled at NODC standard depths.

Some CTD profiles which were not in the SD file and MOODS were also included in the analysis. Those CTD data are readily quality-controlled. No further quality control was done except a re-sample to the NODC standard depths.

A subset of data was selected for the region of the Gulf of Mexico. The hydrocast profiles that were less than 1000 meter depth and/or have less than 10 valid temperature and salinity values were excluded. A total of 2388 hydrocast profiles were available for the analysis. Figure 1 shows the region of study and the spatial distribution. The data were divided into monthly subsets. The number of hydrocasts used at each standard depth is listed by month in Table 1. The monthly mean with root-mean-square (RMS) deviation are shown in Figure 2 for temperature and in Figure 3 for salinity, respectively.

For the following analysis, the temperature and salinity at 19 depths (0, 10, 20, 30, 50, 75, 100, 125, 150, 200, 250, 300, 400, 500, 600, 700, 800, 900, and 1000 meters) were actually used.

3. Empirical Orthogonal Decomposition

From each monthly temperature data set, the covariances, R_{ij} where i and j denoted the depths, were computed,

$$R_{ij} = \frac{1}{K} \sum_{k=1}^{K} \left(T_{ik} - \overline{T}_i\right)\left(T_{jk} - \overline{T}_j\right) \quad i = 1, N; j = 1, N, \tag{1}$$

where N is the number of levels, K is the number of hydrocasts, and $\overline{T}$ is the mean temperature profile. The covariance matrix, $\{R_{ij}\}$, is real and symmetric. Thus, real eigenvectors, Φ_n, and positive eignvalues, λ_n, can be found, such that

$$\sum_{i=1}^{N} R_{ij}\Phi_{ni} = \lambda_n \Phi_{nj}; \quad n = 1, 2, \cdots, N, \tag{2}$$

where the number of modes equals the number of depths. The resulting eigenvectors are orthogonal and are referred to as EOFs. The EOFs of the first three modes are shown in Figure 4.

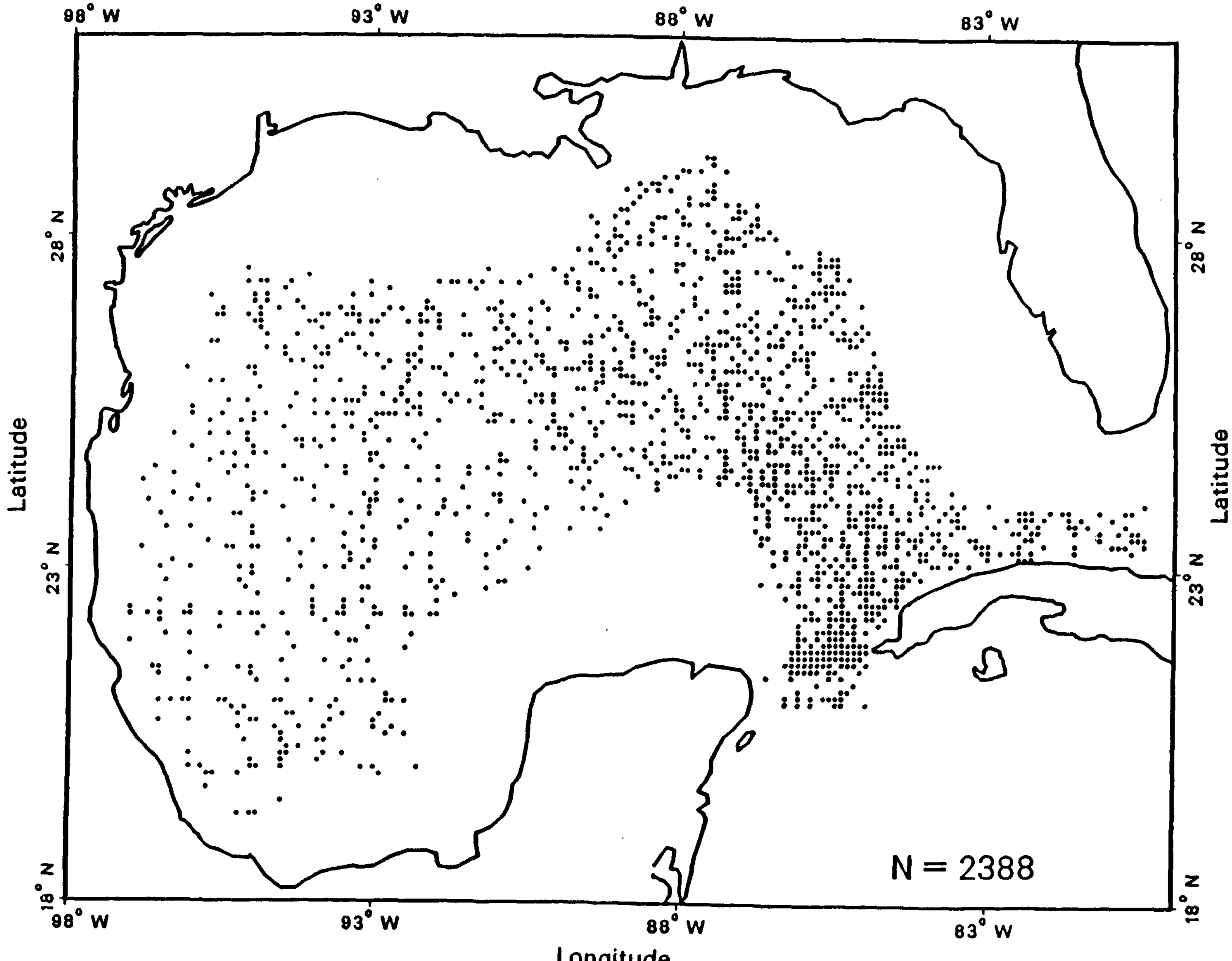

Figure 1. Region of Study and Spatial Distribution of Hydrocast Profiles

LEVEL	DEPTH	JAN	FEB	MAR	APR	MAY	JUN	JUL	AUG	SEP	OCT	NOV	DEC
1	0	101	192	220	167	455	310	64	280	219	145	146	33
2	10	100	191	220	168	456	307	65	282	220	146	149	35
3	20	100	191	220	164	456	307	65	294	223	148	150	35
4	30	100	192	219	165	462	308	66	297	226	151	150	37
5	50	100	192	221	167	466	309	66	301	226	152	152	37
6	75	99	192	223	167	466	310	66	301	226	152	153	37
7	100	98	192	223	167	468	310	66	301	227	152	153	38
8	125	101	192	221	167	467	310	66	298	227	152	152	38
9	150	101	192	219	167	465	309	66	299	228	152	152	38
10	200	102	191	221	165	464	310	66	298	227	153	153	38
11	250	101	190	220	163	465	310	66	298	226	152	153	38
12	300	101	189	217	160	461	310	66	295	226	151	153	38
13	400	100	189	212	158	454	310	65	294	227	145	151	33
14	500	100	189	214	159	454	309	65	296	228	146	152	33
15	600	102	191	222	161	462	310	66	299	229	150	153	36
16	700	102	192	221	163	466	309	66	301	229	151	152	38
17	800	102	190	221	164	467	308	66	301	229	153	152	38
18	900	102	186	217	163	467	308	66	296	229	152	150	38
19	1000	99	172	167	140	407	286	39	247	201	132	130	33

Table 1. Number of Hydrographic Observation

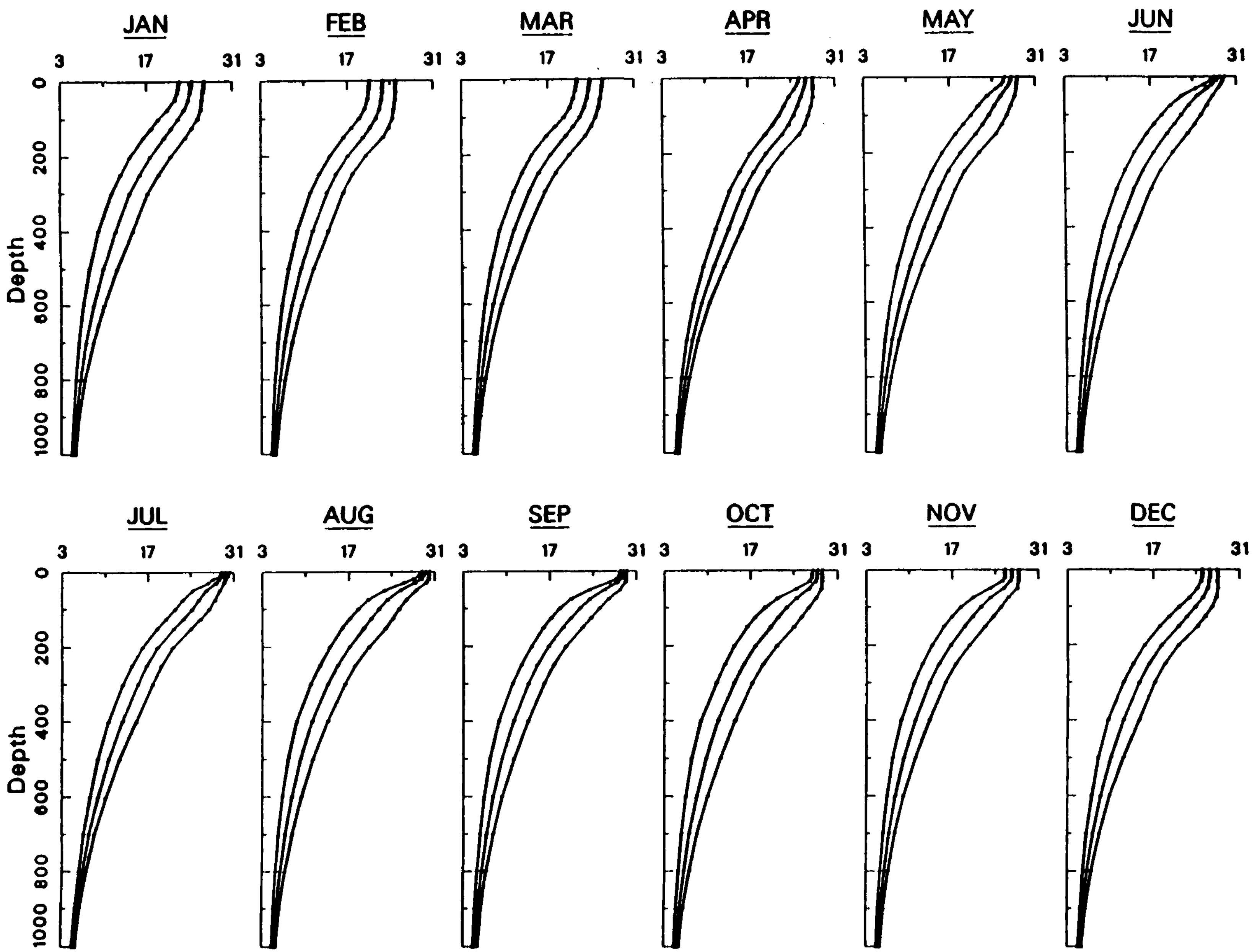

Figure 2. Monthly Mean Temperature with RMS Deviation in Gulf of Mexico

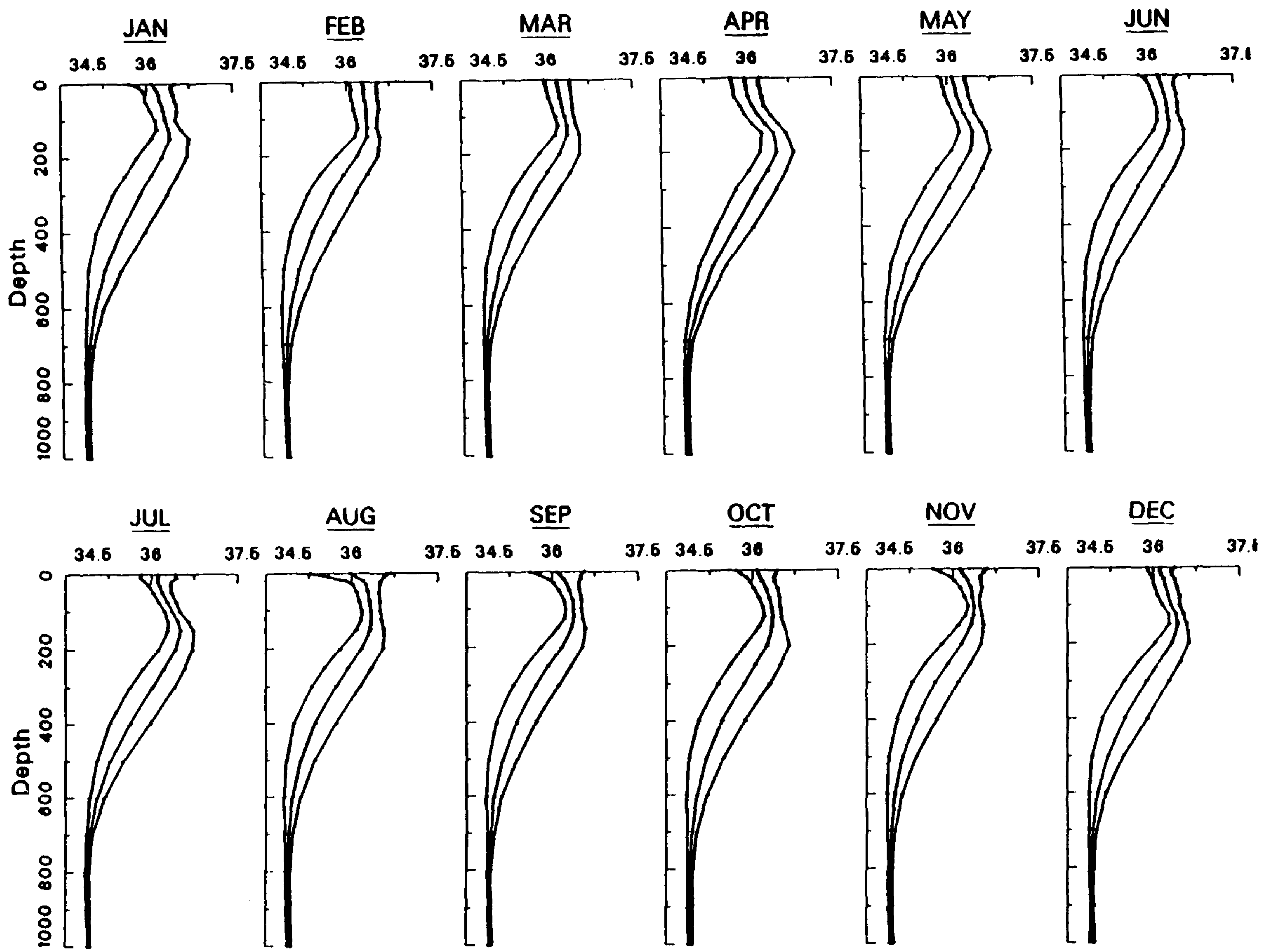

Figure 3. Monthly Mean Salinity with RMS Deviation in Gulf of Mexico

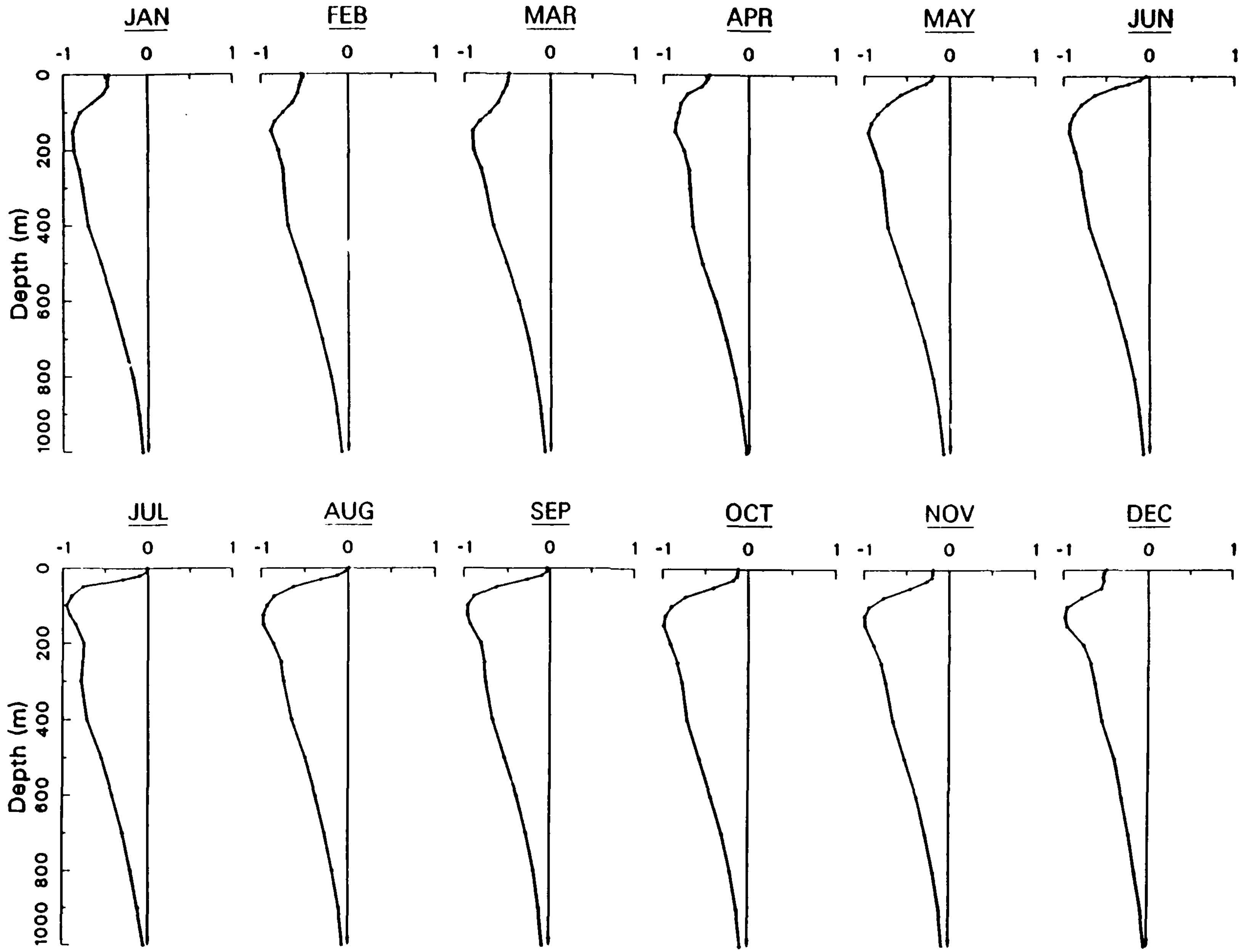

Figure 4a. The Empirical Orthogonal Function (EOF) of the First Mode. The EOFs represent decoupled vertical structure of temperature variations.

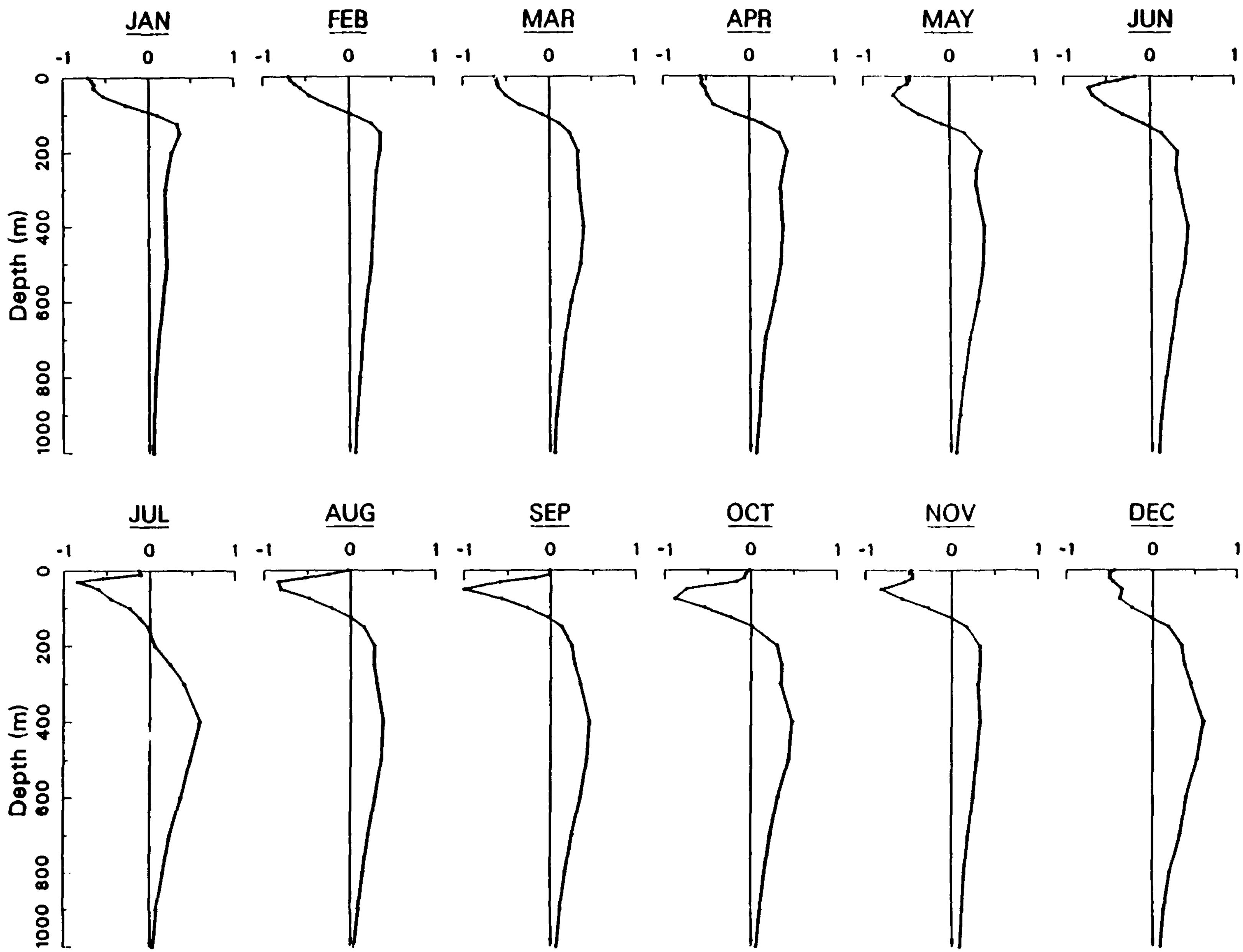

Figure 4b. The Empirical Orthogonal Function (EOF) of the Second Mode.

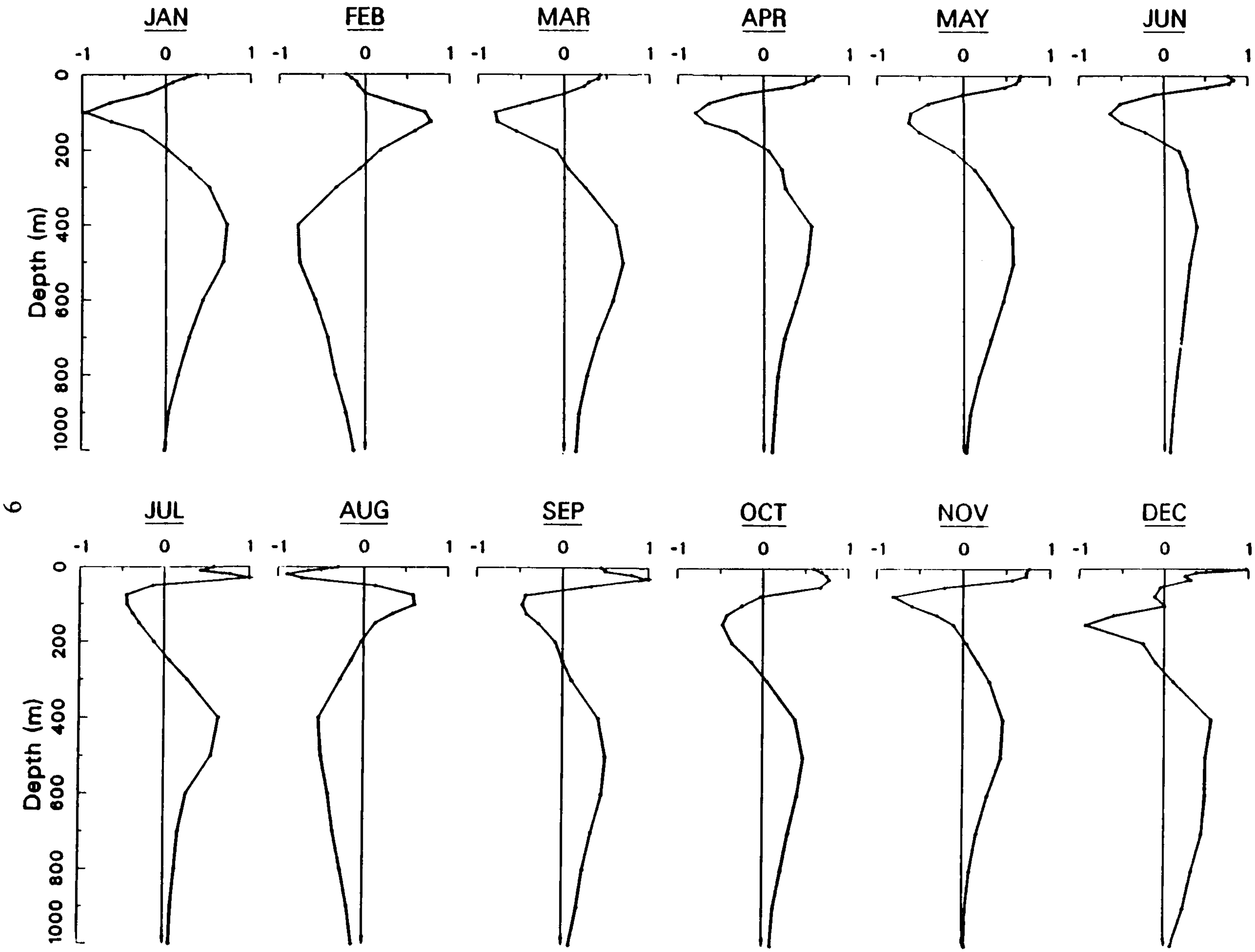

Figure 4c. The Empirical Orthogonal Function (EOF) of the Third Mode.

The contribution of each mode as the proportion of overall variance is determined by the eigenvalues. Table 2 lists the accumulate contribution in percentage. The first two modes account for more than 95 percent of the overall variance in most of the 12 months.

A detailed analysis of the fit by reconstructing the temperature profile using various number of modes, such that

$$T_i = \overline{T}_i + \sum_{n=1}^{M} A_n \Phi_{ni}; \qquad n = 1, 2, \cdots M \text{ and } M \leq N, \tag{3}$$

is presented in Table 3. The misfit represented by the root-mean-square errors (RMSE) is the limit of accuracy which can be achieved by the EOFs accounted for.

4. Statistical Relationship between Dynamic Height and Modal Amplitudes

The relative dynamic heights (0:1000 decibar) were computed according to the hydrostatic equation,

$$\frac{\partial p}{\partial z} = \rho g, \tag{4}$$

where p is pressure, ρ is density, and g is acceleration due to gravity. The amplitudes, A_n, of the first three EOF modes were also computed from cast data,

$$A_n = \sum_{i=1}^{N} \left(T_i - \overline{T}_i\right) \Phi_{ni}; \qquad \text{for } n = 1, 2, 3. \tag{5}$$

A statistical relationship between dynamic height at surface, η, and modal amplitudes was constructed by fitting a third-order polynomial regression equation,

$$A_n = b_{0n} + b_{1n}\eta + b_{2n}\eta^2 + b_{3n}\eta^3, \tag{6}$$

		1 MODE	2 MODE	3 MODE	4 MODE	5 MODE	6 MODE
JAN	:	88.29	95.51	97.44	98.37	98.95	99.29
FEB	:	89.80	96.41	97.95	98.70	99.11	99.40
MAR	:	88.08	95.86	97.96	98.71	99.22	99.53
APR	:	88.37	95.62	97.58	98.48	99.04	99.32
MAY	:	88.31	95.47	97.39	98.09	98.65	99.05
JUN	:	90.28	95.40	97.44	98.18	98.66	99.14
JUL	:	91.18	94.89	97.29	98.33	98.84	99.25
AUG	:	88.68	94.06	96.58	97.85	98.48	98.95
SEP	:	89.96	94.81	97.12	98.23	98.91	99.22
OCT	:	91.12	95.32	97.28	98.27	98.94	99.24
NOV	:	90.07	95.02	97.36	98.27	98.96	99.36
DEC	:	90.97	97.55	98.76	99.30	99.61	99.76

Table 2. The Accumulate Contribution in Percentage.

Depth	RMSE			Bias		
(m)	1 Mode	2 Modes	3 Modes	1 Mode	2 Modes	3 Modes
0 :	1.02	0.37	0.31	-0.01	-0.01	0.00
10 :	0.98	0.30	0.23	0.00	-0.01	0.00
20 :	0.95	0.23	0.17	-0.01	-0.01	-0.01
30 :	0.93	0.20	0.16	-0.02	-0.01	-0.01
50 :	0.85	0.31	0.31	0.00	0.00	0.00
75 :	0.70	0.49	0.41	0.00	0.00	0.00
100 :	0.66	0.66	0.43	0.00	0.00	0.00
125 :	0.70	0.63	0.29	0.02	0.02	0.01
150 :	0.78	0.62	0.40	0.02	0.01	0.01
200 :	0.82	0.60	0.58	0.00	-0.01	-0.01
250 :	0.72	0.47	0.47	0.00	-0.01	-0.01
300 :	0.67	0.43	0.37	0.00	0.00	0.00
400 :	0.81	0.58	0.25	-0.04	-0.02	-0.02
500 :	0.81	0.65	0.35	-0.02	0.00	-0.01
600 :	0.66	0.57	0.42	-0.01	0.00	0.00
700 :	0.48	0.42	0.35	0.00	0.00	0.00
800 :	0.35	0.32	0.28	0.00	0.00	0.00
900 :	0.26	0.24	0.23	0.00	0.00	0.00
1000 :	0.20	0.19	0.18	0.01	0.02	0.02

Table 3. Analysis of the Fit by Reconstructing the Temperature Profile Using Various Number of Modes. The misfit represented by the root-mean-square errors (RMSE) is the limit of accuracy which can be achieved by the EOFs accounted (November shown only).

to the data using least squares. The estimated regressions for the first two EOF modes were shown in Figure 5 for November. The goodness-of-fit represented by R-squared (in percent) is very high for the first mode in every month (listed in Table 4). For the second mode, the goodness-of-fit was much lower and varied each month.

5. Synthetic Temperature Profiles

Based on the derived statistical relationship between dynamic height at surface and modal amplitudes, the synthetic temperature profiles were estimated using simulated sea-surface heights and GEOSAT-measured sea-surface heights. The simulated sea-surface heights were computed from hydrocast data as the relative dynamic height (0:1000 decibar). Results of error analysis of the synthetic temperature profiles from simulated sea-surface heights are listed in Table 5. One section of synthetic temperature profiles along the GEOSAT track (Figure 6) is demonstrated in Figure 7.

6. Summary

The statistical relationship between modal amplitudes and surface dynamic height in the Gulf of Mexico has been investigated. Monthly temperature data were used to determine the EOFs and the modal amplitudes. Temperature and salinity data were applied to computed sea-surface heights (relative dynamic heights). Synthetic temperature profiles were generated using simulated sea-surface heights and the related errors were estimated. Synthetic temperature profiles generated from GEOSAT-measured sea-surface heights were also demonstrated.

7. Acknowledgments

The author wishes to thank Moon-Sik Suk and M.R. Carnes for useful discussions. Aaron Lai assisted in collecting data for the analysis. GEOSAT sea-surface height data were processed by Ziv Sirkes.

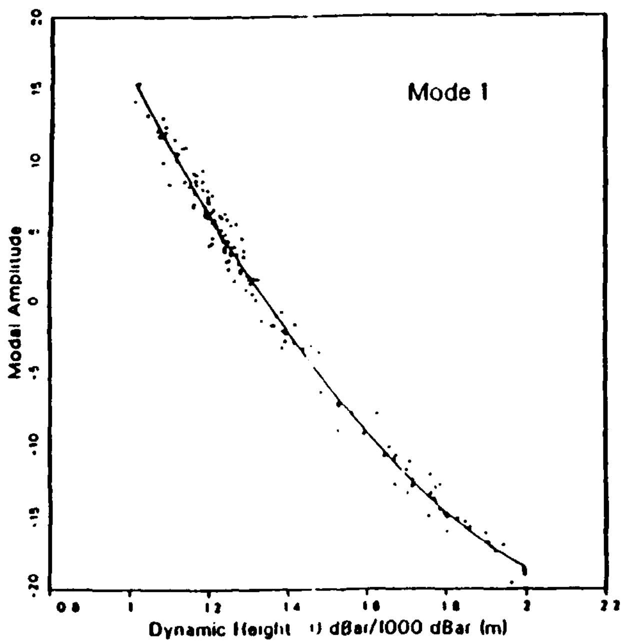

Coefficients	
0	7.1803*10
1	-6.7683*10
2	-3.1160*10
3	4.6476*10

Statistics	
No of Pts	162
Mean of DH	1.38
Mean of MA	-0.017
S D of DH	0.255
S D of MA	8.14
DF Reg	3
R-squared	98.80
DF error	148
RMSE	1.01

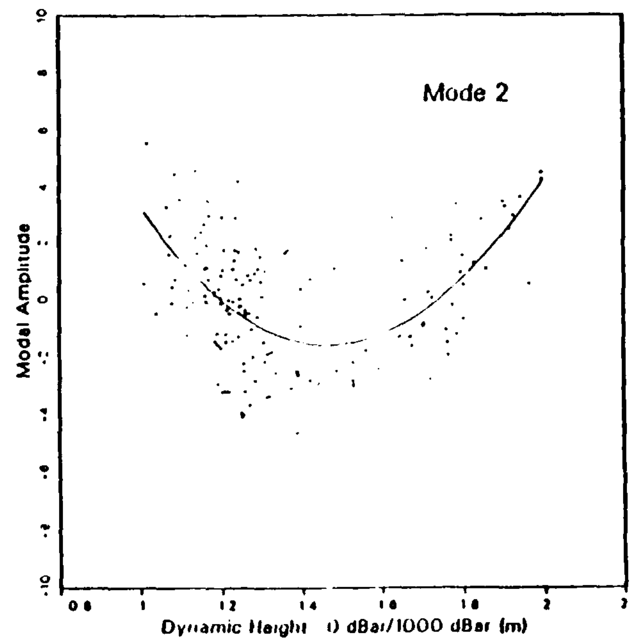

Coefficients	
0	6.1163*10
1	-7.6022*10
2	3.0095*10
3	-1.0032*10

Statistics	
No of Pts	162
Mean of DH	1.38
Mean of MA	-0.008
S D of DH	0.255
S D of MA	2.13
DF Reg	3
R-squared	32.61
DF error	148
RMSE	1.77

Figure 5. Statistical Relationship Between Modal Amplitudes of EOFs and Dynamic Height.

MODE 1

	B0	B1	B2	B3	R2	RMSE	S.D.
JAN :	59.32	-43.21	-8.62	5.57	96.68	1.67	9.02
FEB :	22.39	42.16	-76.80	23.10	98.69	1.04	8.96
MAR :	31.92	25.87	-65.51	20.44	99.11	0.86	9.01
APR :	61.80	-24.47	-29.79	12.01	98.22	1.20	8.89
MAY :	19.47	54.29	-78.80	21.95	98.12	1.21	8.82
JUN :	37.94	9.09	-45.99	14.00	96.43	1.79	9.43
JUL :	48.49	-212.11	199.19	-51.43	98.46	0.99	7.81
AUG :	50.27	-11.52	-34.92	11.89	95.35	1.96	9.07
SEP :	59.30	-24.43	-30.14	11.69	97.37	1.44	8.80
OCT :	-69.84	229.70	-189.49	44.34	98.79	1.05	9.48
NOV :	71.90	-57.58	-3.12	4.65	98.80	1.01	9.14
DEC :	-62.81	231.03	-205.63	51.38	99.13	0.84	8.65

MODE 2

	B0	B1	B2	B3	R2	RMSE	S.D.
JAN :	-68.13	143.68	-98.75	22.18	4.53	2.52	2.54
FEB :	-87.83	200.66	-150.24	36.80	3.10	2.40	2.42
MAR :	-28.77	88.05	-82.38	23.92	16.55	2.42	2.64
APR :	-52.46	138.18	-116.33	31.26	20.37	2.35	2.61
MAY :	39.09	-44.24	2.53	5.83	30.30	2.19	2.61
JUN :	-20.32	70.46	-68.96	20.22	35.82	1.81	2.24
JUL :	157.44	-295.02	178.99	-35.12	37.82	1.29	1.60
AUG :	105.29	-190.52	109.66	-20.02	26.86	1.98	2.30
SEP :	96.68	-178.46	105.12	-19.68	27.77	1.79	2.09
OCT :	84.75	-146.02	78.50	-12.98	35.46	1.65	2.03
NOV :	51.16	-76.02	30.10	-1.90	32.61	1.77	2.13
DEC :	44.99	-53.77	7.39	5.11	38.43	1.90	2.33

Table 4. The Regression Coefficiencies R-Squared (in percent) for the First Two Modes.

Depth	RMSE			Bias		
(m)	1 Mode	2 Modes	3 Modes	1 Mode	2 Modes	3 Modes
0 :	1.08	1.05	1.05	0.00	-0.02	0.01
10 :	1.04	1.01	1.01	0.01	-0.01	0.01
20 :	1.02	0.99	0.99	0.00	-0.02	0.00
30 :	1.00	0.98	0.98	0.00	-0.02	-0.01
50 :	0.93	0.90	0.90	0.02	0.01	0.01
75 :	0.81	0.77	0.77	0.02	0.01	-0.01
100 :	0.77	0.77	0.75	0.02	0.02	-0.02
125 :	0.76	0.77	0.76	0.05	0.05	0.01
150 :	0.82	0.80	0.80	0.04	0.05	0.01
200 :	0.78	0.76	0.76	0.01	0.02	0.01
250 :	0.67	0.67	0.67	0.01	0.02	0.02
300 :	0.61	0.60	0.60	0.01	0.02	0.03
400 :	0.73	0.68	0.66	-0.04	-0.03	0.01
500 :	0.75	0.69	0.67	-0.01	0.00	0.05
600 :	0.60	0.57	0.55	0.00	0.01	0.04
700 :	0.44	0.41	0.40	0.00	0.00	0.03
800 :	0.32	0.31	0.30	0.00	0.00	0.02
900 :	0.24	0.23	0.23	0.01	0.01	0.02
1000 :	0.19	0.19	0.19	0.02	0.02	0.03

Table 5. The Error Analysis of the Synthetic Temperature Profiles From Simulated Sea-Surface Heights (November shown only).

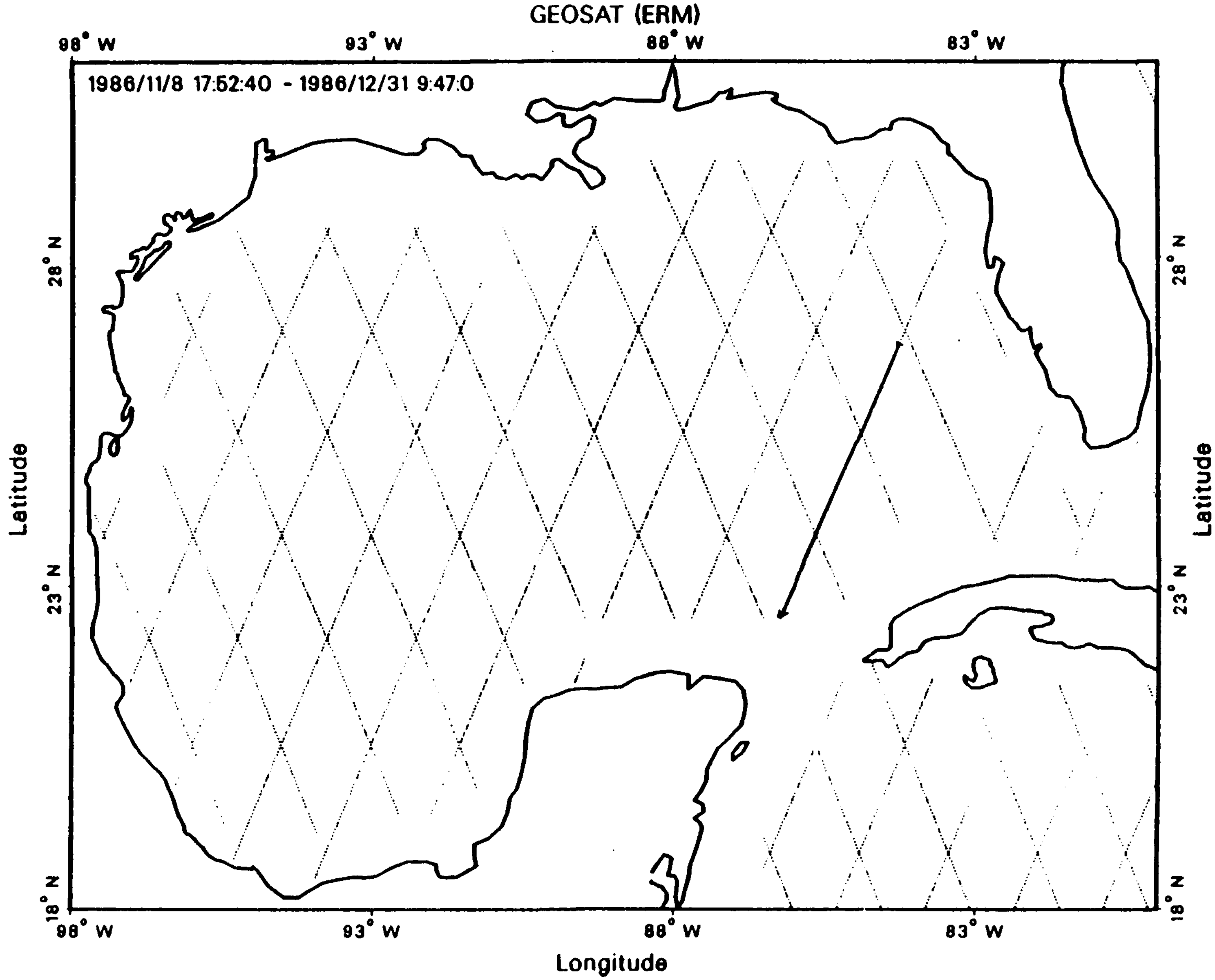

Figure 6. GEOSAT Exact Repeat Mission (ERM) tracks over the Gulf of Mexico. Along track sea-surface height variations (solid line) were used to generate synthetic temperature profiles.

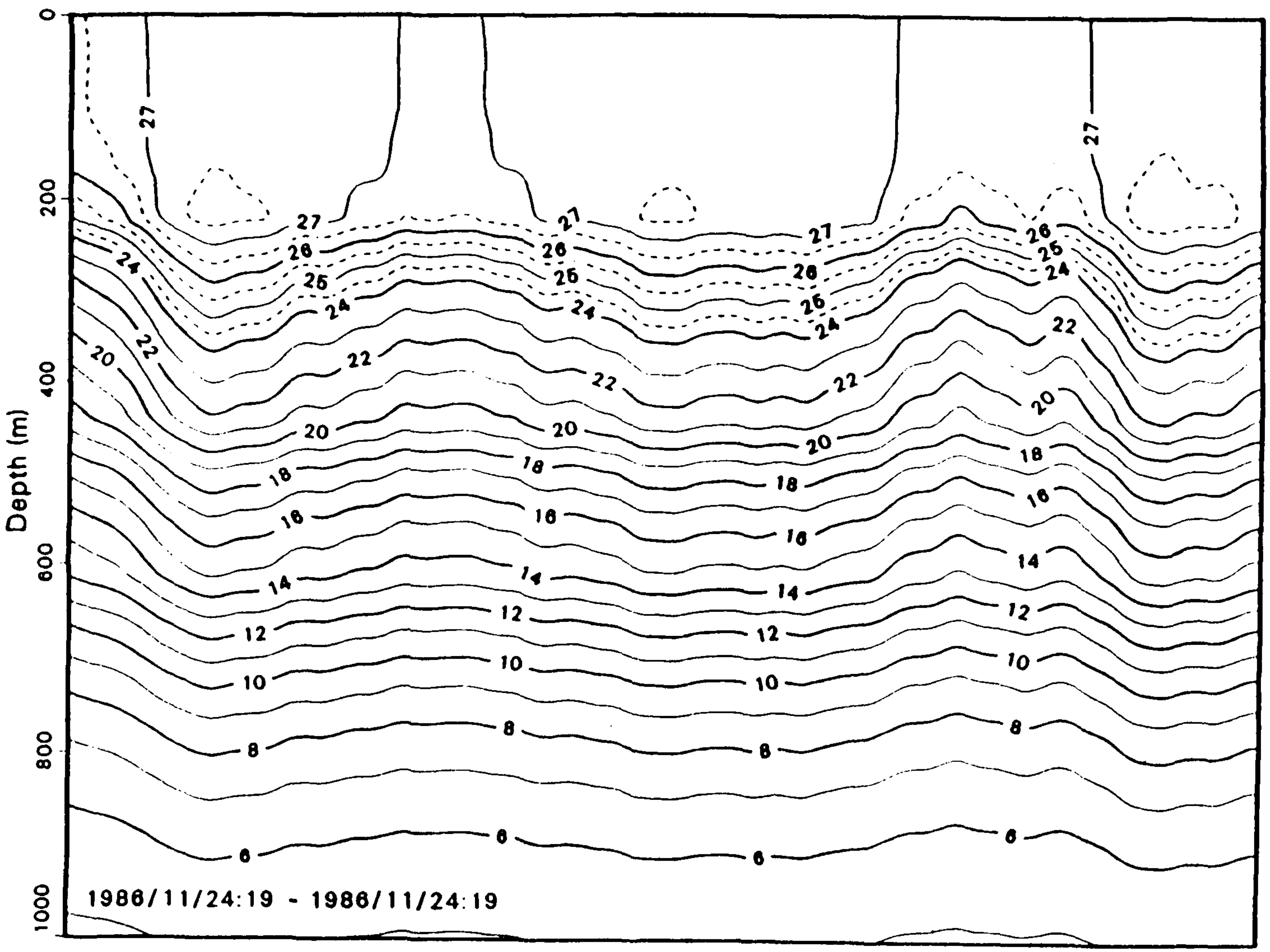

Figure 7. Synthetic Temperature Profiles on a Cross Section Along a GEOSAT ERM Track (Shown by solid line, Figure 6).

8. References

Carnes, M.R., J.L. Mitchell, and P.W. deWitt (1990): Synthetic Temperature Profiles Derived from GEOSAT Altimetry: Comparison with AXBT Profiles, *J. Geophys. Res., 95,* 17, 979-17,992.

Levitus, S. (1982): Climatological Atlas of the World Ocean, *NOAA Professional Paper 13*, U.S. Government Printing Office, Washington, D.C., 173 pp.

deWitt, P.W. (1987): Model Decomposition of Monthly Gulf Stream/ Kuroshio Temperature Fields, *NOO Technical Report 198*, 40 pp.

DISTRIBUTION LIST

1. Office of Naval Research
   Code 1242 (10 copies)
   800 North Quincy Street
   Arlington, VA 22217-5000

2. Director, Atmospheric Sciences
   Directorate
   NRL West (Code 400)
   Monterey, CA 93943-5000

3. Commanding Officer
   Fleet Numerical Oceanography Office
   Monterey, CA 93943-5000

4. Commanding Officer
   Naval Oceanographic Office
   Stennis Space Center, MS 39529

5. Technical Director
   CNOC (Code OOT)
   Stennis Space Center, MS 39529

6. Officer In Charge
   NRL (Code 100)
   Stennis Space Center, MS 39529

7. Technical Director
   NRL (Code 110)
   Stennis Space Center, MS 39529

8. Director, Ocean Sciences
   Directorate
   NRL (Code 300)
   Stennis Space Center, MS 39529

9. Dr. A. D. Kirwan, Jr.
   College of Sciences
   Dept. of Oceanography
   Old Dominion University
   Norfolk, VA 23529-ᴜ276

10. Head, Ocean Sensing and
    Prediction Division
    NRL (Code 320)
    Stennis Space Center, MS 39529

11. Library (3 copies)
    NRL (Code 125)
    Stennis Space Center, MS 39529

12. Dr. William Holland
    National Center for Atmospheric
    Research
    P.O. Box 3000
    Boulder, CO 80307

13. UCAR Library
    P.O. Box 3000
    Boulder, CO 80307

14. Dr. Albert W. Green, Jr.
    NRL, Code 330
    Building 1105
    Stennis Space Center, MS 39529

15. Professor George L. Mellor
    Princeton University
    P.O. Box CN710, Sayre Hall
    Princeton, NJ 08544-0710

16. Dr. John R. Apel
    Applied Physics Laboratory
    Johns Hopkins University
    Laurel, MD 20723

17. Dr. J. Dana Thompson
    NRL, Code 320
    Stennis Space Center, MS 39529

18. Dr. William J. Schmitz
Dept. of Physical Oceanography
Woods Hole Oceanographic Institution
Woods Hole, MA 02543

19. Dr. Edward L. Barker
NRL, Code 440
Monterey, CA 93943-5006

20. Professor Otis B. Brown
Division of Meteorology & Physical Oceanography
RSMAS, University of Miami
4600 Rickenbacker Causeway
Miami, FL 33149

21. Dr. Richard W. Miksad, Chairman
Dept. of Aerospace Engineering and Engineering Mechanics
The University of Texas at Austin
Austin, TX 78712-1085

22. Professor Allan R. Robinson
Center for Earth & Planetary Physics
Harvard University, Pierce Hall
29 Oxford Street, Room 100D
Cambridge, MA 02138

23. Dr. Ron McPherson, Director
National Meteorological Center
World Weather Building
5200 Auth Road
Camp Springs, MD 20746

REPORT DOCUMENTATION PAGE

Form Approved
OMB No. 0704-0188

1. Agency Use Only *(Leave blank).*

2. Report Date.
May 1992

3. Report Type and Dates Covered.
Technical Memo

4. Title and Subtitle.
Synthetic Temperature Profile in the Gulf of Mexico:
Part I. Statistical Relationship Between Model Amplitudes and Dynamic Height at Surface

5. Funding Numbers.
Program Element No. 62435N
Project No. RM35G94
Task No. 801
Accession No. DN250037

6. Author(s).
D. S. Ko

7. Performing Organization Name(s) and Address(es).
Institute for Naval Oceanography
Building 1103, Room 233
Stennis Space Center, MS 39529-5005

8. Performing Organization Report Number.
TM-8

9. Sponsoring/Monitoring Agency Name(s) and Address(es).
Naval Research Laboratory
Stennis Space Center, MS 39529

10. Sponsoring/Monitoring Agency Report Number.

11. Supplementary Notes.

12a. Distribution/Availability Statement.
Approved for public release; distribution is unlimited.

12b. Distribution Code.

13. Abstract *(Maximum 200 words).*

The feasibility of estimating temperature profiles (synthetic temperature profiles) from Geodetic Earth Orbiting Satellite (GEOSAT) altimeter-derived sea-surface heights in the Gulf Stream region has been explored by Carnes et al (1990). The scheme was based on a statistical relationship between sea-surface heights (dynamic height at the surface relative to 1000 dbar) and subsurface temperature profiles derived by deWitt (1987). By analysis of the U.S. Navy's Master Oceanographic Observation Data Set (MOODS) hydrocast data in the Gulf Stream and Kuroshio regions, deWitt found that the first two empirical orthogonal functions (EOFs) of the temperature profiles represented more than 95 percent of the overall temperature variance. Furthermore, he found that there is a tight relationship between relative dynamic height and amplitude of the first two EOF modes. This relationship was used by Carnes et al to generate the synthetic temperature profiles from GEOSAT data. The synthetic temperature profiles compared well with the expendable bathythermograph (XBT) measurements.

In this study the temperature and salinity profiles in the Gulf of Mexico were collected and analyzed. Then the deWitt scheme was employed. The feasibility of using sea-surface heights to estimate temperature profiles (synthetic profiles) in the Gulf of Mexico was investigated.

14. Subject Terms.
(U) INO (U) NAOPS (U) NOGUFS (U) DART (U) SPEM (U) OTIS (U) ECMOP (U) OGCM (U) HARVARD (U) PRINCETON

15. Number of Pages.
23

16. Price Code.

17. Security Classification of Report.	18. Security Classification of This Page.	19. Security Classification of Abstract.	20. Limitation of Abstract.
Unclassified	Unclassified	Unclassified	Unclassified